Research Article

Kinetics, Equilibrium, and Thermodynamics of Methyl Orange Adsorption onto Modified Rice Husk

Chanut Bamroongwongdee*, Saowaluk Gaewkhem and Pongpetch Siritrakul
Department of Industrial Chemistry, Faculty of Applied Science, King Mongkut's University of Technology North Bangkok, Bangkok, Thailand

* Corresponding author. E-mail: chanut.b@sci.kmutnb.ac.th DOI: 10.14416/j.ijast.2018.05.002
Received: 26 April 2017; Accepted: 18 July 2017; Published online: 18 May 2018

Abstract
In this present research, rice husk was modified using a cationic surfactant cetyltrimethylammonium bromide (CTAB) and used as an adsorbent (MRH) to remove methyl orange dye (MO, anionic dye) from aqueous solution. A series of experiments were carried out in a batch process to determine the influences of different parameters such as pH, contact time, initial concentration of adsorbate and adsorbent dose. The kinetic data obtained from different batch experiments were analyzed employing pseudo-first-order, pseudo-second-order, Elovich and intra-particle diffusion model equations. The equilibrium adsorption data were analyzed by Langmuir, Freundlich, Temkin and Dubinin-Radushkevich (D-R) isotherm models. The results show that pseudo-second-order kinetic model and Freundlich adsorption isotherm model achieved better fit with the experimental data. The percent adsorption and equilibrium adsorption capacity (q_e) were increased with the increasing amount of adsorbent and initial concentration of dye, respectively. Thermodynamic parameters such as Gibbs free energy change (ΔG), enthalpy change (ΔH) and entropy change (ΔS) were calculated and the results showed that the adsorption was spontaneous and exothermic.

Keywords: Methyl orange dye, Modified rice husk, Surfactant, Adsorption, Kinetics, Thermodynamics

1 Introduction

With the growth of mankind and technologies, water pollution is one of the most serious problems, especially dye wastewater, for the entire world. The main sources of dye wastewater are the industries that use dyes and pigments to color their products such as leather, textile, fiber, carpet, paper, printing, plastic, ceramic, glass, automotive, food coloring, cosmetics, pharmaceutical and other industries [1]–[6]. Over 7×10^5 ton of dyestuffs are annually produced worldwide and 5–20% of dyes are discharged in the industrial effluents [4]–[6]. Among various industries, textile industry is one of the world's most polluting industries and approximately 100 tons of dyestuffs are discharged into waste streams [5], [6]. The discharge of dye effluents not only affects the aesthetic nature of the environment but also inhibits the photosynthetic activity in the aquatic life by limiting sunlight penetrations [1], [2], [6]–[8].

Usually conventional treatment methods such as precipitation, coagulation and flocculation have been used in the removal of wastewater containing dyes although these techniques do not efficiently remove several common dyes, especially from dilute solutions [9], [10]. An adsorption process is one of the most effective techniques for the removal of dye from the wastewater of textile and dyeing industries because of its simple design and low cost [2], [5], [11]. The activated carbon is widely used as adsorbent because of

Please cite this article as: C. Bamroongwongdee, S. Gaewkhem, and P. Siritrakul, "Kinetics, equilibrium, and thermodynamics of methyl orange adsorption onto modified rice husk," *KMUTNB Int J Appl Sci Technol*, vol. 11, no. 3, pp. 185–197, Jul.–Sep. 2018.

its high adsorption capacity, but its use is limited due to high price of treatment and difficult regeneration [10], [12], [13]. Therefore, many researchers have studied the feasibility of using various low cost materials from agricultural by-products and wastes such as wheat bran [14], magnolia leaf [15], degreased coffee bean [16], mustard husk [17], and peanut husk [18], [19] as adsorbents for the removal of various dyes from the synthetic effluents. However, the effective application of low-cost adsorbents obtained from untreated agricultural by-products or wastes is limited due to presence of net negative surface charge, leading to their low adsorption capacity for anionic pollutants [11], [20]–[22]. Therefore, agricultural by-products need to be modified or treated in a manner to improve their adsorption capacities for anionic pollutants. Recently, some agricultural by-products were modified by cationic surfactant for the removal of anionic ions [20]–[22].

Thailand, an agricultural country, is one of the world's largest producers of rice. Rice Husks (RHs) are agriculture waste materials generated by the rice milling industry. The annual rice production of 20 million ton will produce 5 million ton of husks [23]. The chemical content of RHs consists of cellulose (25–35%), hemicellulose (18–21%), lignin (26–31%), silica (15–17%), solubles (2–5%), and moisture (ca. 7.5%) [24], [25]. RHs can be used as an available adsorbent for the removal of dyes from water and wastewater [10], [13], [26], [27]. However, the investigations using RHs modified by surfactants for removal of anionic dyes from solution were not, in our knowledge, reported in the literature. Hence, in this study, a cationic surfactant, cetyltrimethylammonium bromide (CTAB) was used to modify the surface of RHs to enhance its capacity toward anionic dye from aqueous solution. Methyl Orange (MO) is selected as model anionic azo dye. Azo dyes are widely used in textile, printing, paper, food, colorants, cosmetic, and pharmaceutical industries and are well known to be major human carcinogen [11]. The objective of this study is to study the adsorption property of CTAB modified rice husk towards MO dye. The effects of various factors on the adsorption such as contact time, initial dye concentration, adsorbent dosage, pH and temperature are studied in batch mode. The kinetics, thermodynamics and isotherms of MO removal on the novel materials were investigated.

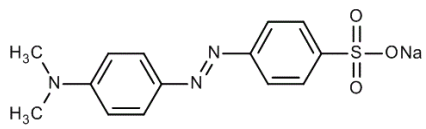

Figure 1: Chemical structure of MO.

2 Materials and Methods

2.1 *Chemicals*

Cetyltrimethylammonium bromide (CTAB) with chemical formula of $C_{19}H_{42}BrN$ and molecular weight of 364.46 g/mol as the surfactant was purchased from Ajax Finechem Pty Ltd. Methyl orange (MO, $C_{14}H_{14}N_3NaO_3S$, molecule weight 327.34 g/mol) was purchased from Fisher Chemical. The chemical structure of MO is illustrated in Figure 1. All other reagents (NaOH and HCl) were of analytical reagent grade and purchased from Ajax Finechem and J.T. Baker, respectively. Distilled water was used for preparing all of the solutions and reagents. The initial pH is adjusted with 0.1 M HCl and NaOH solutions. All the adsorption experiments were carried out at room temperature (30ºC).

A dye stock solution of 1.0 g/L of methyl orange dye was prepared by dissolving the appropriate amount of dye with distilled water. The working solutions were prepared by diluting of the stock solution.

2.2 *Preparation of Modified Rice Husk (MRH)*

The Rice Husk (RH) was collected from local rice mills. The collected materials were washed thoroughly with tap water to remove any adhering dirt, and washed with distilled water, next dried in an oven at 110ºC for 3 h. Dry natural RH was ground and sieved to obtain particle sizes in the range 90–354 μm, then preserved in the desiccator for use.

The synthesis of CTAB modified rice husk was conducted by the following procedure. An amount of 25 g RH was dispersed in 200 mL of aqueous CTAB solution (1wt%), and then the mixture was agitated in shaker machine with 120 rpm at room temperature for 24 h. The Modified Rice Husk (MRH) was then filtered and washed several times with distilled water to remove superficially retained CTAB. Finally, MRH was dried in an oven at 110ºC for 12 h and stored in an airtight glass bottle.

2.3 *Characterization*

The functional groups of the samples were analyzed and interpreted by Fourier transform infrared spectrometer (FTIR-2000, Perkin Elmer) using the potassium bromide (KBr) pellet technique. FTIR spectra were recorded in the range of 4000–400 cm^{-1}.

The pH-zero point of charge (pH_{PZC}) of MRH was determined by the solid addition method, as described in literature [28], [29]. Initial pH of aqueous solutions (pH_i) was adjusted from pH 3 to 11 by adding either 0.1 M HCl or 0.1 M NaOH. 0.2 g of the adsorbents was added to 50 mL of each solution and were keep in equilibrium for 24 h under agitation (120 rpm) at room temperature. The final pH (pH_f) of each aqueous solution was then measured. The difference between the initial and final pH value, $\Delta pH = pH_f - pH_i$, was plotted against the initial pH (pH_i) and the point of intersection of the resulting null ΔpH corresponds to the pH_{PZC}.

2.4 *Batch adsorption studies*

Adsorption experiments were studied in a batch process. The effects of initial MO concentration, contact time, adsorbent amount, and solution pH on the MO uptake were investigated. Sample solutions were shaken in a water-bath shaker at a speed of 120 rpm keeping temperature constant at desire temperature. Samples were withdrawn at desire time, filtered and determined the residual concentrations. The initial and residual concentrations of MO dye were determined by using a UV-Vis Spectrophotometer (Spectronic 20) at a wavelength of maximum absorbance 465 nm.

The amount of dye adsorbed onto MRH at time t, q_t (mg/g), and the percentage removal of MO by MRH, expressed in %R, were calculated using the following Equations (1) and (2):

$$q_t = \frac{(C_0 - C_t)V}{W} \quad (1)$$

$$\%R = \frac{C_0 - C_t}{C_0} \times 100 \quad (2)$$

where C_0 and C_t are the initial dye concentration and the dye concentration at any time t, (mg/L), respectively. V is the volume of dye solution (L), and W is the weight of the adsorbent used (g).

All experiments were carried out by taking known amount of MRH (0.1–1.0 mg) in 250 mL conical flasks containing 50 mL of MO solution of different initial dye concentrations (25–100 mg/L). The pH values of initial MO solutions were adjusted with dilute aqueous solutions of HCl or NaOH (0.1 M). The mixture was shaken in a water-bath shaker at a speed of 120 rpm keeping temperature constant at room temperature (30ºC). The initial and residual concentrations of MO dye were determined by using a UV-Vis Spectrophotometer (Spectronic 20) at a wavelength of maximum absorbance 465 nm.

2.5 *Batch kinetic studies*

Batch kinetic experiments were carried out by taking known amount of MRH in 250 mL conical flasks containing 50 mL of MO solution. The mixture was shaken for various time interval (0–210 min) in a water-bath shaker at a speed of 120 rpm keeping temperature constant at room temperature (30ºC). The samples were withdrawn at different time intervals and the residual concentrations of MO were similarly measured.

2.6 *Batch thermodynamic studies*

The adsorption of MO on MRH was determined as a function of different temperature (30–60ºC) in water-bath shaker under pre-optimized conditions. Various thermodynamic parameters such as Gibbs free energy change (ΔG), enthalpy change (ΔH) and entropy change (ΔS) were calculated.

3 Results and Discussions

3.1 *Characterization of RH and MRH*

The FTIR spectra of RH and MRH were studied in the range of 400–4000 cm^{-1}. It can be seen from Figure 2. FTIR of RH showed that the broad band in the region of 3400 cm^{-1} was due to O–H stretching and indicated the presence of O–H group (carboxylic acids, phenols and alcohols) present in the cellulose, hemicellulose and lignin [11], [18], [30]. The peak at around 2900 cm^{-1} was related to the C–H stretching vibrations of the bonds in $–CH_3$ and CH_2 groups in the structure of rice

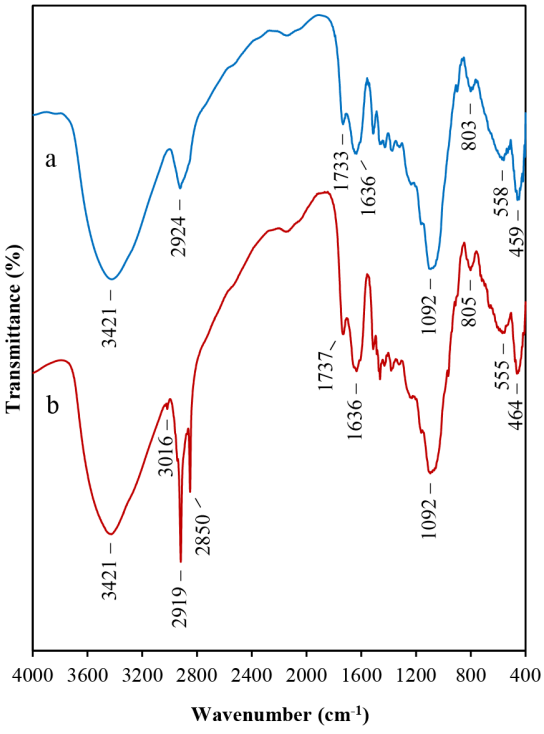

Figure 2: Fourier transform infrared spectroscopy spectra of a – Rice Husk (RH) and b – CTAB Modified Rice Husk (MRH).

husk biomass. The weak adsorption band at 1733 cm^{-1} corresponds to the C=O stretching vibrations. The intense adsorption band at 1636 cm^{-1} was related to the deformation vibrations of water molecules. The intense band at 1092 cm^{-1} was considered to result from the stretching vibrations of Si–O tetrahedrons. The small peak at 803 cm^{-1} can be attributed to the stretching vibration of the Si–O bonds. The adsorption band appeared at 459 cm^{-1} corresponded to the bending vibration of siloxane bonds (Si–O) [30].

In comparison with the spectrum of RH, that of MRH shows more intense adsorption bands at 2919 and 2850 cm^{-1}, which is due to the symmetric and asymmetric stretching vibrations of methyl group ($–CH_3$) and the methylene ($–CH_2$) of the aliphatic chain of the surfactant [8], [20]. Furthermore, the new adsorption band in spectrum of MRH was observed around 3016 cm^{-1}, which is ascribed to the stretching vibration of CH_3–N [8]. These clearly indicate that natural RH has been successful modified by CTAB.

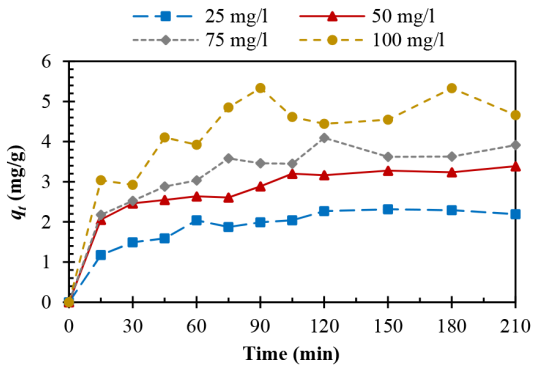

Figure 3: Effect of contact time and initial MO dye concentration on the MO adsorption onto MRH.

3.2 *Adsorption performance in batch mode*

3.2.1 Effect of initial dye concentration/contact time

The effects of initial dye concentration and contact time on MO dye adsorption are shown in Figure 3. Initially, the adsorption of MO dye increased rapidly, but it gradually slowed down until it reached a plateau. At the initial stage, the adsorption rate was rapid due to the availability of readily accessible surface sites. After a lapse of time, the remaining surface sites were gradually decreased as equilibrium reached [12], [13], [28]. Another reason was that dye molecules were adsorbed on the exterior surface of the adsorbent. After complete adsorption on the exterior surface, the dye molecules were adsorbed in the interior surface of the adsorbent particles [13], [14], [17].

From Figure 3, the increase in the initial MO concentration led to proportional increase in the adsorption uptakes of dye at equilibrium and this may be due to the enhanced driving force of mass transfer at higher initial dye concentration [5], [12], [28]. Figure 3 also shows that the adsorption of MO dye reached equilibrium in about 120 min, although the data were taken for 210 min. The equilibrium adsorption capacity (q_e) was found to be 2.3 mg/g for 25 mg/L of initial MO concentration, this value was 5.3 mg/g for that of 100 mg/L.

3.2.2 Effect of adsorbent dosage

The percentage removal and equilibrium adsorption capacity of MO onto MRH are shown in Figure 4. The

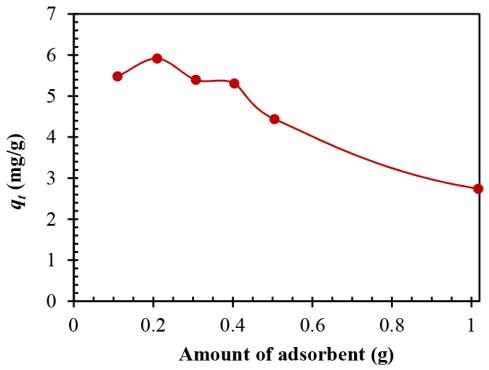

Figure 4: Effect of adsorbent mass on the MO adsorption onto MRH.

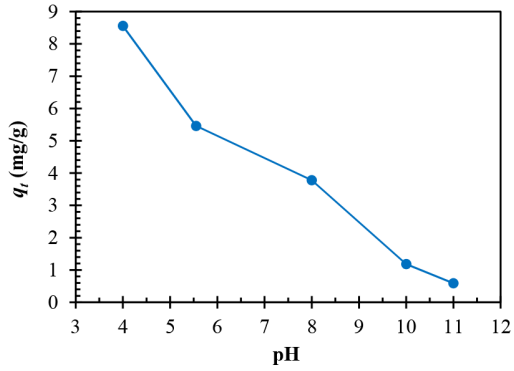

Figure 5: Effect of initial pH on the adsorption of MO on MRH.

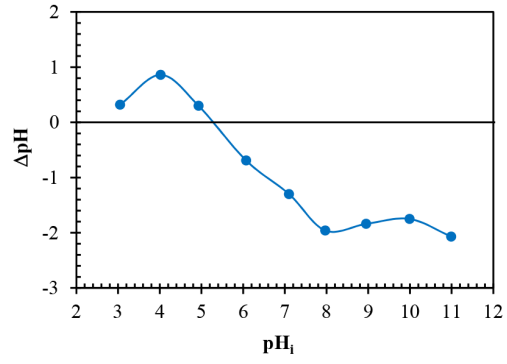

Figure 6: Point of zero charge of MRH.

results showed that the biosorption capacity of MRH decreased with the increase in biomass concentration. The dye uptake decreased from 5.76 to 2.74 mg/g for an increase in adsorbent mass from 0.1 to 1.0 g. The decrease in biosorption capacity of MRH with increasing adsorbent mass might be due to the split in the MO concentration gradient between the solution and the adsorbent surface. Therefore, the amount of MO adsorbed onto unit mass of MRH was decreased with increasing MRH mass [4], [31], [32].

3.2.3 Effect of pH and zero point charge (pH_{PZC})

The initial pH of the dye solution is one of the most important factors in all the adsorption processes especially for dye adsorption [5], [11], [33]–[35]. The influence of the initial pH on the MO removal using MRH was studied in the pH ranging from 4 to 11 and the results are shown in Figure 5. A pH less than 4.0 could not be investigated due to color change of dye solution [36]. It was observed that the equilibrium adsorption capacity remarkably decreased with an increase in pH of the initial solution. These results could be described by the different electrostatic interaction between MO and MRH surface in terms of surface charge and degree of dye dissociation. In acidic conditions, the MRH surface becomes more positively charged, which enhanced the anionic MO molecule through the electrostatic forces of attraction. Furthermore, the higher adsorption of dye at acidic pH (as in Figure 5) is probably due to the protonation of sulfonate groups of MO from $–SO_3^-$ to $–SO_3H$. At a high pH solution, the number of anionic forms (sulfonate groups dissociated, $–SO_3$) of MO were increased and led to a decrease in the electrostatic repulsion. Also, the competition between OH^- and the anionic sulfonate groups for positively charged adsorption sites increased with the increase in the solution pH which caused the decrease in adsorption rate.

The effect of the solution pH could be further explained on the basis of zero point of charge (pH_{PZC}), which is the point at which the net surface charge of the adsorbent surface is zero. The pH_{PZC} of MRH was determined to be 5.3 (see Figure 6). In principle, when the solution pH < pH_{PZC}, the MRH surface becomes positively charge and the adsorption of anionic dye is favorable due to the electrostatic force of attraction increased. For solutions with pH > pH_{PZC}, the MRH surface becomes negatively charged, thus making OH^- ions compete effectively with the dye anions causing a decrease in the uptake of anionic dye. This observation

is in agreement with data reported in the literature [5], [13], [17].

3.3 *Adsorption isotherm*

To optimize the adsorption mechanism pathways for adsorption of adsorbate, it is essential to establish the most appropriate correlation for the equilibrium data. In this study, several models of the adsorption isotherm like those of Langmuir, Freundlich, Temkin, and Dubinin-Radushkevich (D-R) have been employed to investigate the adsorption behaviour. The applicability of isotherm equations to the adsorption study within the experimental conditions (concentration range 25–100 mg/L, adsorbent dose 4 g/L, temperature 30ºC, contact time 210 min and stirring speed 120 rpm) was compared by judging the correlation coefficient values, R^2. The higher R^2 value implies a better fit with a maximum R^2 value of 1.0.

3.3.1 Langmuir isotherm

The Langmuir isotherm model can be presented in the following relation [11], [33] [Equation (3)]:

$$q_e = \frac{q_m K_L C_e}{\left(1 + K_L C_e\right)} \tag{3}$$

where q_e (mg/g) is the amount of dyes adsorbed at equilibrium time, C_e (mg/L) is the equilibrium concentration of dye solution, q_m (mg/g) is the maximum adsorption capacity describing a complete monolayer adsorption and K_L (L/mg) is the Langmuir isotherm constants related to the free energy or enthalpy of adsorption. The linearized form of Langmuir isotherm can be written as [Equation (4)]:

$$\frac{C_e}{q_e} = \frac{1}{q_m K_L} + \frac{1}{q_m} C_e \tag{4}$$

A plot of C_e/q_e against C_e gave the best fitted curve indicating that the adsorption process did not follow this model [Figure 7(a)]. The values of q_m, K_L and correlation coefficient (R^2) obtained from the Langmuir plot are given in Table 1. The significant characteristics of the Langmuir isotherm can be expressed in terms of the dimensionless constant separation factor, R_L, defined by [12], [31], [34] [Equation (5)]:

$$R_L = \frac{1}{1 + K_L C_0} \tag{5}$$

where C_0 (mg/L) is the initial dye concentration. The R_L value indicates the type of the adsorption to be either unfavorable ($R_L > 1$), linear ($R_L = 1$), favorable ($0 < R_L < 1$) or irreversible ($R_L = 0$) [31], [34]. The calculated R_L values for all dye concentrations were in the range of 0–1, showing that the entire adsorption processes were favourable.

Table 1: Parameters of adsorption models for MO adsorption onto MRH

Isotherm Model	Parameter	MRH
Langmuir	q_m (mg/g)	5.99
	K_L (L/mg)	0.035
	R_L	0.535
	R^2	0.997
Freundlich	n	2.127
	K_F (mg/g)	0.597
	R^2	0.987
Temkin	A	0.254
	B	1.515
	R^2	0.987
D-R	q_{mD-R} (mg/g)	5.321
	β_{D-R} (mol^2/kJ^2)	6.103
	E (kJ/mol)	0.286
	R^2	0.978

3.3.2 Freundlich isotherm

The Freundlich adsorption isotherm model can be expressed as [11], [33] [Equation (6)]:

$$q_e = K_F C_e^{1/n} \tag{6}$$

where q_e (mg/g) is the amount of dye adsorbed at equilibrium, C_e (mg/L) is the equilibrium concentration of dye solution, K_F (mg/g) is the Freundlich adsorption constant related to the adsorption capacity, and n is the constant indicative of the intensity of the adsorption processes. In general, the value of n lying in the range of 1 to 10 illustrates that the adsorbate is favorably adsorbed on the adsorbent. The numerical number of n less than 1 indicates that the adsorption process is chemical in nature. The Freundlich equation can be

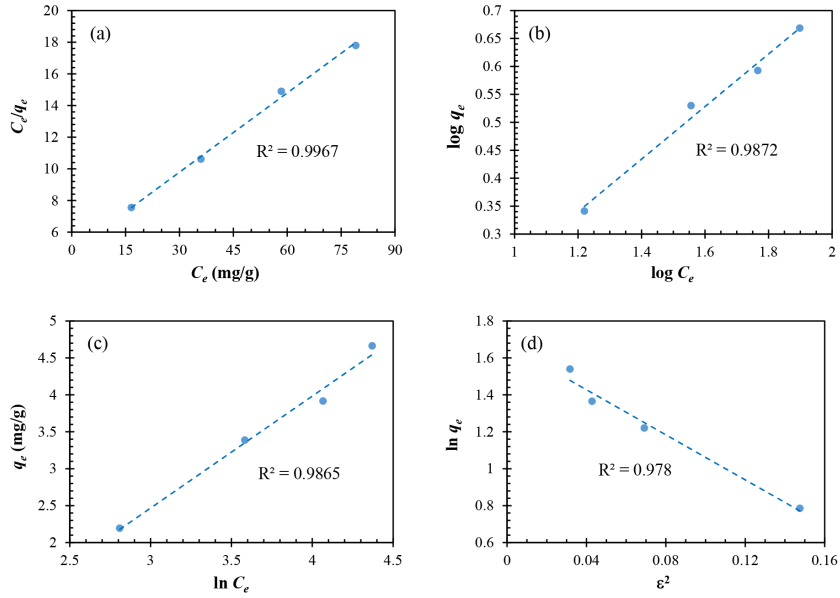

Figure 7: Equilibrium adsorption data fitted to the (a) Langmuir isotherm, (b) Freundlich isotherm, (c) Temkin isotherm and (d) Dubinin-Radushkevich isotherm.

converted to a linear form by taking logarithms of both sides as [Equation (7)]:

$$\log q_e = \log K_F + \frac{1}{n}\log C_e \tag{7}$$

A plot of log q_e against log C_e produces a straight line of slope 1/n and intercept log K_F [Figure 7(b)]. The values of the Freundlich equilibrium coefficients K_F and n were generated from the plot of sorption data (see Table 1). The parameter n found in the range of 1 to 10, which proves that the adsorption is favorable and process is physical in nature.

3.3.3 Temkin isotherm

The Temkin isotherm assumes that the heat of adsorption of all the molecules in the layer would drop linearly with increasing surface coverage due to adsorbent-adsorbate interaction and the adsorption is characterized by a uniform distribution of binding energies [28]. The Temkin model [11], [12] is expressed as [Equation (8)]:

$$q_e = B\ln A + B\ln C_e \tag{8}$$

where q_e (mg/g) is the experimental adsorption capacity at equilibrium, C_e (mg/L) is the concentration of dyes adsorbed at equilibrium, A (L/mg) is the equilibrium binding constant corresponding to the maximum binding energy and B (J/mol) is the Temkin constant related to the heat of adsorption and is given as [Equation (9)]:

$$B = \frac{RT}{b_T} \tag{9}$$

where $1/b_T$ indicates the adsorption potential of the adsorbent, R (8.314 J/mol.K) is the universal gas constant and T (K) is the absolute temperature.

A plot of q_e against ln C_e gives a linear graph with B as the slope and B(ln A) as the intercept [Figure 7(c)]. The results of this isotherm parameters are displayed in Table 1.

3.3.4 Dubinin–Radushkevich (D–R) isotherm

The Dubinin-Radushkevich model [11], [13] is used to describe the adsorption in microporous materials. This model is more general than the Langmuir isotherm because it does not assume a homogeneous surface or constant adsorption potential. The linear form of the D–R isotherm Equation (10) is:

$$\ln q_e = \ln q_m - \beta\varepsilon^2 \quad (10)$$

where q_e (mg/L) is the amount of dye molecules, q_m (mg/g) is the theoretical saturation capacity, β (mol^2/kJ^2) is the activity coefficient related to the mean free energy of adsorption and ε is the Polanyi potential which can be correlated to temperature as [Equation (11)]:

$$\varepsilon = RT \ln\left(1 + \frac{1}{C_e}\right) \quad (11)$$

where R (kJ/mol.K) is the gas constant, and T (K) is the absolute temperature. The adsorption mean free energy E (kJ/mol) can be calculated as follows [Equation (12)]:

$$E = \frac{1}{\sqrt{2\beta}} \quad (12)$$

The mean free energy gives information about the type of adsorption mechanism. If the value of E is in the range of 8 to 16 kJ/mol, the sorption process is governed by chemical ion-exchange, and if the values of $E < 8$ kJ/mol, the sorption is a physical in nature. The plot of ln q_e against ε^2 is employed to determine the β and q_m from the slope and the intercept respectively [Figure 7(d)]. The calculated values of the D–R parameters are shown in Table 1. The value of the free energy estimated from the D–R model is lower than 8 kJ/mol, indicating that the adsorption of MO onto MRH was physical adsorption in nature.

The theoretical parameters for all the isotherms studied are listed in Table 1. By comparing the value of correlation coefficient, it can be concluded that the Langmuir isotherm is the best-fit isotherm for the adsorption of MO onto MRH.

3.4 *Adsorption kinetic study*

In order to examine the controlling mechanisms of sorption process such as chemical reaction, diffusion control and mass transfer, several kinetic models are used to analyse experimental data from the adsorption of MO onto MRH. Therefore, pseudo-first-order, pseudo-second-order, Elovich, and intra-particle diffusion kinetic models were used for the adsorption of MO onto MRH. The applicability of these kinetic models was compared by judging the correlation coefficients R^2.

3.4.1 Pseudo-first-order model

The pseudo-first-order model of Lagergren [37] has been widely used to predict the dye sorption kinetics and its formula is given as [Equation (13)]:

$$\frac{dq_t}{dt} = k_1\left(q_e - q_t\right) \quad (13)$$

where q_t (mg/g) and q_e (mg/g) denote the adsorption capacities at any time t (min) and at the equilibrium time, respectively, k_1 (1/min) is the rate constant of the pseudo-first-order adsorption and t (min) is the contact time. Integrating the above equation for the boundary conditions $t = 0$ to $t = t$ and $q_t = 0$ to $q_t = q_t$, leads to [Equation (14)]:

$$\log\left(q_e - q_t\right) = \log q_e - \frac{k_1}{2.303}t \quad (14)$$

The slope and intercept can be derived from the plot of log $(q_e - q_t)$ against t, which is usually to determine the first-order rate constant k_1, equilibrium adsorption density q_e and correlation coefficient R^2 [Figure 8(a)]. It was found that the R^2 value obtained for the pseudo-first-order kinetic model did not show a consistent trend and a large difference existed between the calculated ($q_{e,\,cal}$) and experimental ($q_{e,\,exp}$) adsorption capacity value (see Table 2). Therefore, the adsorption of MO on MRH did not followed the pseudo-first-order kinetic model.

3.4.2 Pseudo-second-order model

The differential form of the pseudo-second-order kinetic model could be expressed as [38] [Equation (15)]:

$$\frac{dq_t}{dt} = k_2\left(q_e - q_t\right)^2 \quad (15)$$

where k_2 (g/mg.min) is the rate constant of the pseudo-second-order adsorption. The integrating of the above equation with the boundary conditions $t = 0$ to $t = t$ and $q_t = 0$ to $q_t = q_t$, could be rearranged in the linear form as follows [Equation (16)]:

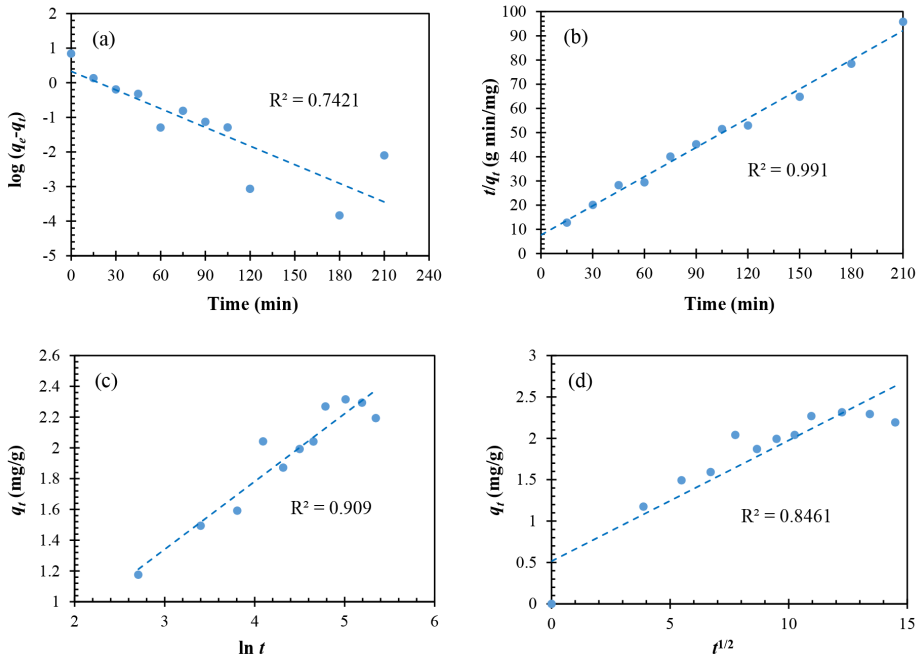

Figure 8: (a) Pseudo-first-order kinetics, (b) pseudo-second-order kinetics, (c) Elovich kinetics and (d) intra-particle diffusion kinetics for the adsorption of MO onto MRH adsorbent.

$$\frac{t}{q_t} = \frac{1}{k_2 q_e^2} + \frac{1}{q_e} t \tag{16}$$

The rate constant k_2 was calculated from the intercept of the plot of t/q_t against t [Figure 8(b)]. The R^2 value of the pseudo-second-order model was close to unity, which was much higher than the R^2 value of the pseudo-first-order model (Table 2). Furthermore, the calculated q_e value for the pseudo-second-order model was closer to the experimental q_e value. It can be concluded that the pseudo-second-order model provided a good correlation for the adsorption of MO onto MRH.

3.4.3 Elovich model

The Elovich model equation can be expressed as [39] [Equation (17)]:

$$\frac{dq_t}{dt} = a \exp(-bq_t) \tag{17}$$

where a (mg/g.min) is the initial adsorption rate and b (g/mg) is related to the extent of surface coverage and activation energy for chemisorption. Integrating of the above equation, assuming $abt >> 1$ and applying the boundary conditions $t = 0$ to $t = t$ and $q_t = 0$ to $q_t = q_t$, is simplified to [Equation (18)]:

$$q_t = \frac{1}{b} \ln(ab) + \frac{1}{b} \ln t \tag{18}$$

The values of the initial adsorption rate, a, and desorption constant, b, were determined from the intercept and slope of the linear plot of q_t versus ln t [Figure 8(c)]. The data obtained by the Elovich model are given in Table 2. The value of correlation coefficient is higher than 0.9, which indicated that the adsorption of MO on MRH can be described by the Elovich model.

3.4.4 Intra-particle diffusion model

The biosorption process involves the movement of dye molecules (absorbate) from the aqueous solution to the biosorbent surface. The mechanism of biosorption of dye molecules on biosorbent may be controlled by single step or a series of steps. In the batch system, film diffusion or/and intra-particle diffusion may be

the rate-limiting step [1], [13]. Therefore, the kinetic results were analyzed by using the intra-particle diffusion model proposed by Weber and Morris [40]. The initial rate of intra-particle diffusion model can be described as [Equation (19)]:

$$q_t = k_{id}\sqrt{t} + C \tag{19}$$

where $\sqrt{t}$ (min) is the half-life time, k_{id} (mg/g.min$^{0.5}$) is the rate constant of intra-particle diffusion and C (mg/g) is the intercept of a plot of q_t versus $\sqrt{t}$ which describes the boundary layer thickness. If the value of C is equal to zero, the intra-particle diffusion is the only rate-limiting step and the larger the value of C the greater the effect of the boundary layer. The kinetic parameters and the correlation coefficient R^2 are listed in Table 2. The value of C in intra-particle is not zero and the value of the correlation coefficient R^2 is less than 0.9 [Figure 8(d)]. Therefore, it can be concluded that the intra-particle diffusion is not the only rate-limiting step and the biosorption of MO onto MRH did not followed the intra-particle diffusion model.

Table 2: Kinetic parameters for adsorption of MO (25 mg/L) onto MRH

Kinetic Model	Parameter	MRH
Pseudo-first-order	$q_{e,exp}$ (mg/g)	2.32
	$q_{e,cal}$ (mg/g)	2.15
	k_1 (1/min)	0.042
	R^2	0.742
Pseudo-second-order	$q_{e,cal}$ (mg/g)	2.49
	k_2 (g/mg.min)	0.021
	R^2	0.991
Elovich	a	0.459
	b	2.267
	R^2	0.909
Intra-particle diffusion	C	0.517
	k_{id} (mg/g.min$^{0.5}$)	0.146
	R^2	0.846

3.5 *Thermodynamic parameters*

To estimate the effect of temperature on the adsorption of MO onto MRH, thermodynamic parameters, such as the Gibbs free energy ΔG, enthalpy change ΔH, and entropy change ΔS, were determined.

The values of ΔG at different temperature were determined by the following Equation (20):

$$\Delta G = -RT \ln K_C \tag{20}$$

where R (8.314 J/mol.K) is the universal gas constant, T (K) is the absolute temperature and K_C is the adsorption equilibrium constant, which is the ratio of the equilibrium concentration of MO adsorbed to the equilibrium concentration of MO in solution.

The values of ΔH and ΔS can then be calculated by using the linear form of the Van't Hoff Equation (21):

$$\ln K_C = -\frac{\Delta G}{RT} = -\frac{\Delta H}{R}\frac{1}{T} + \frac{\Delta S}{R} \tag{21}$$

The plot of ln K_C versus 1/T yields a straight line from which the values of ΔH and ΔS were calculated from the slope and intercept, respectively.

The calculated values of ΔH, ΔS and ΔG for the adsorption of MO on MRH are represented in Table 3. The values of ΔG can be given an idea about the type of adsorption, whether it is a physisorption ($-20 < \Delta G < 0$ kJ/mol) or chemisorption ($-400 < \Delta G < -80$ kJ/mol) [11], [31]. From Table 3, the values of ΔG are negative for all cases, and are within the range of –20 to 0 kJ/mol, indicating that the adsorption of MO onto MRH is feasible and spontaneous physical process. The negative value of ΔH indicates that the adsorption of MO onto MRH is exothermic in nature. The magnitude of ΔH may also be used to indicate the type of adsorption force (i.e., van der Waals forces 4–10 kJ/mol, hydrophobic bond forces about 5 kJ/mol, hydrogen-bonding forces 2–40 kJ/mol, dipole-dipole interaction 2–29 kJ/mol, dentate exchange about 40 kJ/mol, and chemical bond forces > 60 kJ/mol) [11], [31], [41]. The value of ΔH suggests that hydrogen-bonding and dipole-dipole interaction may contribute to the adsorption process in addition to electrostatic attraction. The negative value of ΔS reflects the decrease in randomness at the solid/solution interface during adsorption of MO onto MRH and the affinity of the adsorbent for dye.

Table 3: Thermodynamic parameters for the adsorption of MO (100 mg/L) onto MRH

T (°C)	ΔG^0 (kJ/mol)	ΔH^0 (kJ/mol)	ΔS^0 (J/mol.K)
30	–2.201	–19.897	–58.403
40	–1.617		
50	–1.033		
60	–0.449		

4 Conclusions

This study shows that modified rice husk by cationic surfactant, CTAB, is a promising adsorbent for removal of anionic dye, methyl orange, from aqueous solution in the batch mode. The adsorption capacity increases as the initial MO concentrations increases, and as dosage dose and solution pH decrease. The kinetic data showed that the pseudo-second-order kinetic model agrees very well with the dynamic adsorption behavior of MO onto MRH. The isothermal data were found to be the best described by the Langmuir isotherm. The thermodynamic data revealed that the adsorption process was spontaneous and exothermic in nature. The mechanism for the adsorption of MO on the MRH may involve the different types of electrostatic interactions including dipole-dipole and hydrogen-bonding force.

Acknowledgments

The authors would like to express their gratitude to the Department of Industrial Chemistry and Faculty of Applied Science (general research grant no. 6041104), King Mongkut's University of Technology North Bangkok (KMUTNB) for the financial support.

References

[1] K. S. Bharathi and S. T. Ramesh, "Removal of dyes using agricultural waste as low-cost adsorbents: A review," *Applied Water Science*, vol. 3, no. 4, pp. 773–790, 2013.

[2] G. Karaçetin, S. Sivrikaya, and M. Imamoğlu, "Adsorption of methylene blue from aqueous solutions by activated carbon prepared from hazelnut husk using zinc chloride," *Journal of Analytical and Applied Pyrolysis*, vol. 110, pp. 270–276, 2014.

[3] M. P. Tavlieva, S. D. Genieva, V. G. Georgieva, and L. T. Vlaev, "Kinetic study of brilliant green adsorption from aqueous solution onto white rice husk ash," *Journal of Colloid and Interface Science*, vol. 409, pp. 112–122, 2013.

[4] M. T. Yagub, T. K. Sen, and H. M. Ang, "Equilibrium, kinetics, and thermodynamics of methylene blue adsorption by pine tree leaves," *Water, Air, & Soil Pollution*, vol. 223, no. 8, pp. 5267–5282, 2012.

[5] M. T. Yagub, T. K. Sen, S. Afroze, and H. M. Ang, "Dye and its removal from aqueous solution by adsorption: A review," *Advances in Colloid and Interface Science*, vol. 209, pp. 172–184, 2014.

[6] Y. Zhang, L. Bai, W. Zhou, R. Lu, H. Gao, and S. Zhang, "Superior adsorption capacity of Fe_3O_4@nSiO_2@mSiO_2 core-shell microspheres for removal of congo red from aqueous solution," *Journal of Molecular Liquids*, vol. 219, pp. 88–94, 2016.

[7] V. S. Munagapati and D.-S. Kim, "Adsorption of anionic azo dye congo red from aqueous solution by cationic modified orange peel powder," *Journal of Molecular Liquids*, vol. 220, pp. 540–548, 2016.

[8] M. A. Zenasni, B. Meroufel, A. Merlin, and B. George, "Adsorption of congo red from aqueous solution using CTAB-kaolin from bechar algeria," *Journal of Surface Engineered Materials and Advanced Technology*, vol. 4, pp. 332–341, 2014.

[9] T. K. Saha, "Adsorption of methyl orange onto chitosan from aqueous solution," *Journal of Water Resource and Protection*, vol. 2, no. 10, pp. 898–906, 2010.

[10] P. Sharma, R. Kaur, C. Baskar, and W. J. Chung, "Removal of methylene blue from aqueous waste using rice husk and rice husk ash," *Desalination*, vol. 259, no. 1–3, pp. 249–257, 2010.

[11] R. Lafi and A. Hafiane, "Removal of methyl orange (MO) from aqueous solution using cationic surfactants modified coffee waste (MCWs)," *Journal of the Taiwan Institute of Chemical Engineers*, vol. 58, pp. 424–433, 2016.

[12] M. A. Ahmad and N. K. Rahman, "Equilibrium, kinetics and thermodynamic of Remazol Brilliant Orange 3R dye adsorption on coffee husk-based activated carbon," *Chemical Engineering Journal*, vol. 170, no. 1, pp. 154–161, 2011.

[13] Y. Safa and H. N. Bhatti, "Kinetic and thermodynamic modeling for the removal of Direct Red-31 and Direct Orange-26 dyes from aqueous solutions by rice husk," *Desalination*, vol. 272, no. 1–3, pp. 313-322, 2011.

[14] S. Ata, M. Imran Din, A. Rasool, I. Qasim, and I. Ul Mohsin, "Equilibrium, thermodynamics, and kinetic sorption studies for the removal of coomassie brilliant blue on wheat bran as a low-cost adsorbent," *Journal of Analytical Methods*

in Chemistry, vol. 2012, pp. 405980, 2012.

[15] H. Yu, T. Wang, L. Yu, W. Dai, N. Ma, X. Hu, and Y. Wang, "Remarkable adsorption capacity of Ni-doped magnolia-leaf-derived bioadsorbent for congo red," *Journal of the Taiwan Institute of Chemical Engineers*, vol. 64, pp. 279–284, 2016.

[16] M.-H. Baek, C. O. Ijagbemi, S.-J. O, and D.-S. Kin, "Removal of Malachite Green from aqueous solution using degreased coffee bean," *Journal of Hazardous Materials*, vol. 176, no. 1–3, pp. 820–828, 2010.

[17] R. K. Gautam, A. Mudhoo, and M. C. Chattopadhyaya, "Kinetic, equilibrium, thermodynamic studies and spectroscopic analysis of Alizarin Red S removal by mustard husk," *Journal of Environmental Chemical Engineering*, vol. 1, no. 4, pp. 1283–1291, 2013.

[18] S. Sadaf and H. N. Bhatti, "Batch and fixed bed column studies for the removal of Indosol Yellow BG dye by peanut husk," *Journal of the Taiwan Institute of Chemical Engineers*, vol. 45, no. 2, pp. 541–553, 2014.

[19] S. Sadaf and H. N. Bhatti, "Evaluation of peanut husk as a novel, low cost biosorbent for the removal of Indosol Orange RSN dye from aqueous solutions: Batch and fixed bed studies," *Clean Technologies and Environmental Policy*, vol. 16, no. 3, pp. 527–544, 2014.

[20] H. Chen, J. Zhao, J. Wu, and G. Dai, "Isotherm, thermodynamic, kinetics and adsorption mechanism studies of methyl orange by surfactant modified silkworm exuviae," *Journal of Hazardous Materials*, vol. 192, no. 1, pp. 246–254, 2011.

[21] Y. Su, B. Zhao, W. Xiao, and R. Han, "Adsorption behavior of light green anionic dye using cationic surfactant-modified wheat straw in batch and column mode," *Environmental Science and Pollution Research*, vol. 20, no. 8, pp. 5558–5568, 2013.

[22] R. D. Zhang, J. H. Zhang, X. N. Zhang, C. C. Dou, and R. P. Han, "Adsorption of Congo red from aqueous solutions using cationic surfactant modified wheat straw in batch mode: Kinetic and equilibrium study," *Journal of the Taiwan Institute of Chemical Engineers*, vol. 45, no. 5, pp. 2578–2583, 2014.

[23] C. Santasnachok, W. Kurniawan, and H. Hinode, "The use of synthesized zeolites from power plant rice husk ash obtained from Thailand as adsorbent for cadmium contamination removal from zinc mining," *Journal of Environmental Chemical Engineering*, vol. 3, no. 3, pp. 2115–2126, 2015.

[24] P. Leiva, E. Ciannamea, R. A. Ruseckaite, and P. M. Stefani, "Medium-density particleboards from rice husks and soybean protein concentrate," *Journal of Applied Polymer Science*, vol. 106, no. 2, pp. 1301–1306, 2007.

[25] L. Ludueña, D. Fasce, V. A. Alvarez, and P. M. Stefani, "Nanocellulose from rice husk following alkaline treatment to remove silica," *BioResources*, vol. 6, no. 2, pp. 1440–1453, 2011.

[26] S. Chakraborty, S. Chowdhury, and P. Das Saha, "Adsorption of Crystal Violet from aqueous solution onto NaOH-modified rice husk," *Carbohydrate Polymers*, vol. 86, no. 4, pp. 1533–1541, 2011.

[27] S. Chowdhury, R. Mishra, P. Saha, and P. Kushwaha, "Adsorption thermodynamics, kinetics and isosteric heat of adsorption of malachite green onto chemically modified rice husk," *Desalination*, vol. 265, no. 1–3, pp. 159–168, 2011.

[28] K. Y. Foo and B. H. Hameed, "Coconut husk derived activated carbon via microwave induced activation: Effects of activation agents, preparation parameters and adsorption performance," *Chemical Engineering Journal*, vol. 184, pp. 57–65, 2012.

[29] S. Kaur, S. Rani, and R. K. Mahajan, "Adsorption kinetics for the removal of hazardous dye congo red by biowaste materials as adsorbents," *Journal of Chemistry*, vol. 2013, pp. 12, 2013.

[30] S. D. Genieva, S. Ch. Turmanova, A. S. Dimitrova, and L. T. Vlaev, "Characterization of rice husks and the products of its thermal degradation in air or nitrogen atmosphere," *Journal of Thermal Analysis and Calorimetry*, vol. 93, no. 2, pp. 387–396, 2008.

[31] S. G. Liu, Y. Q. Ding, P. F. Li, K. S. Diao, X. C. Tan, F. H. Lei, Y. H. Zhan, Q. M. Lib, B. Huang, and Z. Y. Huang, "Adsorption of the anionic dye Congo red from aqueous solution onto natural zeolites modified with N,N-dimethyl dehydroabietylamine oxide," *Chemical Engineering Journal*, vol. 248, pp. 135–144, 2014.

[32] P. S. Kumar, S. Ramalingam, C. Senthamarai, M. Niranjanaa, P. Vijayalakshmi, and S. Sivanesan,

"Adsorption of dye from aqueous solution by cashew nut shell: Studies on equilibrium isotherm, kinetics and thermodynamics of interactions," *Desalination*, vol. 261, no. 1, pp. 52–60, 2010.

[33] R. Katal, M. S. Baei, H. T. Rahmati, and H. Esfandian, "Kinetic, isotherm and thermodynamic study of nitrate adsorption from aqueous solution using modified rice husk," *Journal of Industrial and Engineering Chemistry*, vol. 18, no. 1, pp. 295–302, 2012.

[34] L. Lin, S.-R. Zhai, Z.-Y. Xiao, Y. Song, Q.-D. An, and X.-W. Song, "Dye adsorption of mesoporous activated carbons produced from NaOH-pretreated rice husks," *Bioresource Technology*, vol. 136, pp. 437–443, 2013.

[35] Q.-Q. Zhong, Q.-Y. Yue, Q. Li, X. Xu, and B.-Y. Gao, "Preparation, characterization of modified wheat residue and its utilization for the anionic dye removal," *Desalination*, vol. 267, no. 2–3, pp. 193–200, 2011.

[36] A. Dutta and R. K. Dutta, "Fluorescence behavior of cis-methyl orange stabilized in cationic premicelles," *Spectrochimica Acta Part A: Molecular and Biomolecular Spectroscopy*, vol. 126, pp. 270–279, 2014.

[37] S. Langergren, "About the theory of so-called adsorption of soluble substances," *Kungliga Svenska Vetenskapsakademiens Handlingar*, vol. 24, pp. 1–39, 1898.

[38] Y. S. Ho and G. McKay, "Pseudo-second order model for sorption processes," *Process Biochemistry*, vol. 34, no. 5, pp. 451–465, 1999.

[39] J. Zeldowitsch, "Über den mechanismus der katalytischen oxydation von CO an MnO_2," *Acta Physicochimica U.R.S.S.*, vol. 1, pp. 364–449, 1934.

[40] W. J. Weber and J. C. Morris, "Kinetics of adsorption on carbon from solution," *Journal of the Sanitary Engineering Division*, vol. 89, no. 2, pp. 31–60, 1963.

[41] T. Qiu, Y. Zeng, C. Ye, and H. Tian, "Adsorption thermodynamics and kinetics of p-Xylene on activated carbon," *Journal of Chemical & Engineering Data*, vol. 57, no. 5, pp. 1551–1556, 2012.